Title

The spread of herpes simplex virus type 1 from trigeminal neurons to the murine cornea: an immunoelectron microscopy study

Journal

Journal of Virology, 74(10)

Authors

Ohara, Peter T
Chin, Marian S
LaVail, Jennifer H

Publication Date

2003

Peer reviewed

JOURNAL OF VIROLOGY, May 2000, p. 4776–4786 Vol. 74, No. 10
0022-538X/00/$04.00+0

The Spread of Herpes Simplex Virus Type 1 from Trigeminal Neurons to the Murine Cornea: an Immunoelectron Microscopy Study

PETER T. OHARA,[1,3] MARIAN S. CHIN,[1]† AND JENNIFER H. LAVAIL[1,2,3]*

Departments of Anatomy[1] and Ophthalmology[2] and the Neuroscience Program,[3] University of California, San Francisco, San Francisco, California 94143

Received 28 December 1999/Accepted 25 February 2000

An animal model has been developed to clarify the mechanism for spread of herpes simplex virus (HSV) from neuron to epithelial cells in herpetic epithelial keratitis. HSV was introduced into the murine trigeminal ganglion via stereotaxic guided injection. After 2 to 5 days, the animals were euthanized. Ganglia and corneas were prepared for light and electron microscopic immunocytochemistry with antisera to HSV. At 2 days, labeled axons were identified in the stromal layer. At 3 days, we could detect immunoreactive profiles of trigeminal ganglion cell axons that contained many vesicular structures. By 3 and 4 days, the infection had spread to all layers of epithelium, and the center of a region of infected epithelium appeared thinned. At 5 day, fewer basal cells appeared infected, although infection persisted in superficial cells where it had expanded laterally. Mature HSV was found in the extracellular space surrounding wing and squamous cells. Viral antigen was expressed in small pits along the apical surfaces of wing and squamous cells but not at the basal surface of these cells or on basal cells. This polarized expression of viral antigen resulted in the spread of HSV to superficial cells and limited lateral spread to neighboring basal cells. The pathogenesis of HSV infection in these mice may serve as a model of the human recurrent epithelial disease in the progression of focal sites of infection and transfer from basal to superficial cells.

Herpes simplex virus (HSV) keratitis, one of the leading causes of infectious corneal blindness in humans (14, 29), involves a two-step process of infection and reinfection. Initially, HSV type 1 replicates in the mucous membranes of the mouth or corneal epithelium, where sensory and autonomic nerve terminals take it up. Virus is transported in a retrograde direction to sensory ganglion cell bodies. Although many ganglion neurons support a lytic infection, a subpopulation of neurons supports an HSV infection in which the virus remains latent. The second phase of corneal infection follows from viral reactivation in the latently infected ganglion cells of the trigeminal ganglion. After anterograde transport to the eye, new virus can be found in tears and in the corneal epithelium and stroma. With repeated reactivation cycles, the corneal stroma become progressively more scarred, with resulting decrease in vision and other ocular complications including glaucoma, iritis and cataract, and even necrotizing retinitis (8).

During the past 30 years, the molecular basis of HSV neurovirulence and neuroinvasiveness in the eye has been studied intensively (see references 22 and 30 for reviews). However, our understanding of how reactivated virus is transported in sensory axons and how it is released to the cornea is limited. One reason for the slow progress rests on the lack of an effective animal model with which to investigate the steps of spread of reactivated virus from neuron to cornea. Most previous animal models have depended on delivery of virus via a scarified cornea (see references 13 and 25 for reviews). The major limitation of that approach is that there is no way to separate the confounding components of retrograde transport of virus to the trigeminal ganglion, anterograde transport back to cornea, and potential reactivation of virus in latently infected corneal cells. The alternative cell culture approach used by several groups of investigators (6, 18) has also attempted to address several of these questions, but the anterograde transport of HSV in sensory neurons in vivo remains to be investigated.

What has been needed is an experimental system in which HSV can be applied directly to the relevant trigeminal ganglion cells and the subsequent transport and release of newly synthesized virus to corneal epithelium can be assayed over time. With such an assay, one could address questions about the period of time required for sufficient viral replication, the morphology of the anterograde-transported particle, the relative susceptibility of corneal epithelial cell types to infection, and the viral and cellular proteins that are essential for this behavior.

The strategy used in this study has been to introduce HSV directly into the mouse trigeminal ganglion and trace the spread of virus from neuron cell bodies to axon terminal fields in the cornea and from there spread in the corneal epithelium (Fig. 1). We have chosen this route of introduction of HSV for several reasons. The viral inoculum can be accurately controlled, the time course of infection and subsequent spread to the cornea can be defined, and the potential contribution of reactivated virus from other sites, such as the autonomic ganglia or even the corneal epithelium (2), can be eliminated. Initially, we have chosen to study the spread between neurons and corneal cells in an immunologically naive host, to concentrate on the effects of viral pathogenesis and to minimize the immunopathogenic effect that would normally occur during viral reactivation.

Using this model, we have found that infection and transport of virus can mimic human corneal herpetic infection by trigeminal ganglion axons with no accessory contribution of infection of autonomic ganglia. We have found that the spread of virus from corneal cell to cell occurs in a polarized fashion and involves primarily the wing and squamous cells, with little con-

* Corresponding author. Mailing address: Box 0452, Department of Anatomy, University of California, San Francisco, 513 Parnassus Ave., San Francisco, CA 94143-0452. Phone: (415) 476-1694. Fax: (415) 476-4845. E-mail: jhl@itsa.ucsf.edu.

† Present address: Immunology and Virology Section, National Eye Institute, National Institutes of Health, Bethesda, MD 20892-1857.

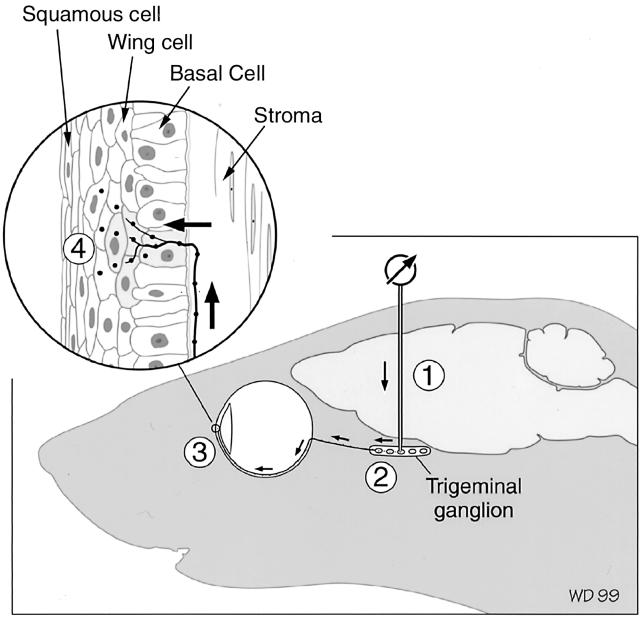

FIG. 1. Diagram to illustrate the site of inoculation of virus into the trigeminal ganglion. The micropipette was directed to the area of the trigeminal ganglion that supplies innervation to the cornea, using stereotaxic coordinates and by recording receptive field responses from the skin around the eye (1). Trigeminal ganglion neurons take up the virus (2) and transport it to the cornea (3). (Inset) An axon in the subbasal plexus (arrow) enters the epithelium and releases virus to infect epithelial cells (4). Three histologically distinguishable cell layers (squamous, wing, and basal cell layers) comprise the epithelium.

tribution of the basal cells of the epithelium or underlying stromal cells. The spread of virus from neuronal terminal to corneal epithelial cells mimics the pattern of spread in the human recurrent epithelial disease (26).

MATERIALS AND METHODS

Propagation of viral stocks. African green monkey kidney (Vero) cells were grown in high-glucose Dulbecco's modified Eagle's medium supplemented with 10% fetal bovine serum, nonessential amino acids, and penicillin-streptomycin at 37°C. Cells grown to 80% confluency were infected with 0.001 PFU of F strain HSV (designated YBH-Mp3) per cell in DME H21 containing 1% fetal bovine serum, nonessential amino acids, and penicillin-streptomycin. After 48 h, the medium and extracellular virus were collected. All of the following steps were performed at 4°C. Cellular debris was removed by centrifugation at 3,000 rpm for 10 min using a Sorvall GSA rotor, and virus was pelleted by centrifugation of the supernatant using an SW28 rotor (Beckman Instruments, Inc. Palo Alto, Calif.) at 12,000 rpm for 90 min. For viral stocks, the resulting pellets were resuspended in minimal essential medium containing 5% (wt/vol) bovine serum albumin, aliquoted, and stored at −80°C.

Inoculation of trigeminal ganglia. All procedures with animals adhered to the Society for Neuroscience guidelines for the use of animals in research and the guidelines of the UCSF Committee on Animal Research. Twenty-six 6- to 8-week-old male BALB/c mice were injected with HSV in the left trigeminal ganglion. The animals were first anesthetized with an intraperitoneal injection of Avertin (17) and placed in a stereotaxic head holder. An incision was made in the skin over the left cranium, and a small opening was made in the cranium. Glass electrodes (outside diameter, 1.2 mm; inside diameter, 0.5 mm) that had been pulled to a tip diameter of 20 μm were backfilled with the viral solution. The electrode was mounted in a picospritzer electrode carrier (General Valve Corporation, Fairfield, N.J.) and lowered through the left cerebral cortex with a stereotaxic manipulator to the approximate coordinates of the trigeminal ganglia. Final placement of the electrode was determined by recording whisker and corneal receptive fields via the injection electrode and monitored with an oscilloscope and audio monitor. When corneal receptive fields (and therefore the region that supplies axons to the cornea) were located, the picospritzer was used to inject the viral solution (2×10^9 to 3×10^9 PFU/ml) (Fig. 1). Only the initial animal in a series of injections was used for recording; the remaining animals were injected at those coordinates. To determine the volume and titer of virus injected from the picospritzer, we deposited an equivalent amount of virus into media and then titered the amount of infective virus on Vero cell plates. Based on this control experiment, we estimate that volumes of about 1 to 1.3 μl were injected.

Immunocytochemistry. After trigeminal inoculation with HSV, the mice were allowed to survive 2 ($n = 3$), 3 ($n = 4$), 4 ($n = 6$), or 5 ($n = 8$) days. The mice were anesthetized with Halothane and euthanized by intracardiac perfusion with saline followed by 4% paraformaldehyde in phosphate buffer (pH 7.2). The brainstem, left and right trigeminal ganglia, and right and left corneas were dissected and prepared for immunocytochemistry according to standard procedure (12). Horizontal sections from the trigeminal ganglia and transverse sections of the brainstems from the level of the superior colliculus to the first cervical segments of the spinal cord were cut at 30-μm thickness on a cryostat, and the sections were collected in phosphate-buffered saline. Corneas were either prepared as whole mounts or cut on a cryostat approximately perpendicular to the surface of the cornea in 10-μm-thick sections. The corneas or corneal and trigeminal sections were first incubated overnight in blocking solution composed of 3% normal goat serum and 0.1% Triton X-100 in phosphate-buffered saline (pH 72). The following day, the sections were incubated in primary antiserum (horseradish peroxidase-conjugated polyclonal antiserum raised in rabbits against human HSV-1; 1:100 dilution; Accurate Chemical & Scientific Corp. Westbury, N.Y.), and the presence of HSV antigens was determined with diaminobenzidine (DAB) as the substrate according to standard methods (12). Whole mounts were incubated according to the nickel-DAB (Ni-DAB) reaction (15). As controls, the right corneas and trigeminal ganglia of the same animals were reacted with the anti-HSV antiserum and substrate.

EM immunocytochemistry. We prepared material for electron microscopic (EM) immunocytochemistry to determine the subcellular distribution of HSV antigen. An additional nine mice were inoculated with HSV as described above and allowed to survive 2 ($n = 2$), 3 ($n = 4$), 4 ($n = 1$), or 5 ($n = 2$) days. The mice were anesthetized and perfused through the heart with a fixative composed of 4% paraformaldehyde and 0.1% glutaraldehyde followed by a second fixative composed of paraformaldehyde, lysine, and sodium metaperiodate (20) in cacodylate buffer (pH 7.2). After 2 h, the corneas and trigeminal ganglia were dissected and treated for immunocytochemistry as whole cornea or ganglia according to procedures described above. After reaction with Ni-DAB (15), the corneas were osmicated in reduced osmium (9), stained with 2% uranyl acetate, dehydrated, and flat embedded between sheets of Aclar film (Polysciences, Inc., Warrington, Pa.) for EM. Thin sections were cut, poststained with lead citrate and uranyl acid, and examined and photographed with an electron microscope. The left corneas of these mice as well as corneas from two additional uninoculated mice were also prepared as controls for the EM study. Using electron micrographs taken at magnifications ranging from ×30,000 to ×50,000, we measured with a digitizer the diameters of immunostained viral particles in axons, in the nucleus, and free in the cytoplasm or surrounded by a cellular membrane. The mean and standard deviation were calculated.

RESULTS

Trigeminal ganglion. The trigeminal ganglion contains the cell bodies of the sensory neurons that supply the neuronal innervation to most of the head. The portion of the ganglion that innervates the cornea and conjunctiva is located in the rostromedial quadrant of the ganglion (19). Twenty-six of the 35 mice received virus in the appropriate region of the left trigeminal ganglion. The distance the virus spread from the injection site varied with the time after infection. In the animals that were euthanized only 2 days after infection, we found HSV-immunoreactive cells in a region about 1 mm in radius around the pipette tract. The mice with successful injections developed blepharitis and keratitis in the left eye at about 4 days following inoculation of HSV into the left trigeminal ganglion. The right eye remained consistently clear of infection. No HSV-positive cells were identified in control trigeminal ganglia. No signs of eye disease were observed in the remaining mice in which virus was delivered outside of the location of neurons that projected to the central cornea.

By 2 days after viral inoculation, we found evidence of uptake and replication of virus in trigeminal ganglion neurons at the site of injection (Fig. 2A and B). The infected neurons included those that were histologically normal with lightly immunoreactive cytoplasm and darkly reacted nuclei, as well as frankly degenerated, vacuolated ganglion cells (Fig. 2B). In areas of the ganglion more distant from the pipette tract, we found only uninfected cells that appeared cytologically normal and had no reaction product. These cells resembled those of

Trigeminal Ganglion

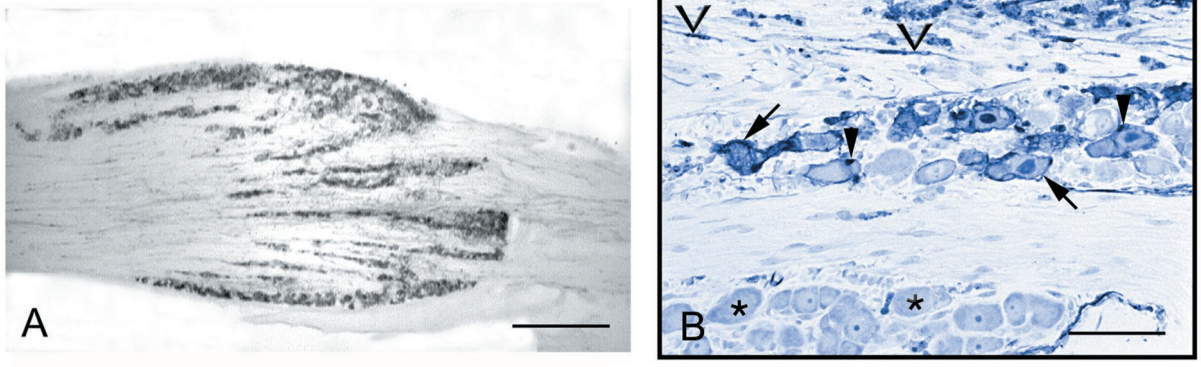

Trigeminal Axons

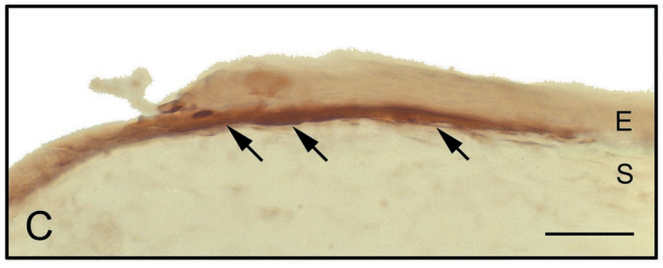

Cornea

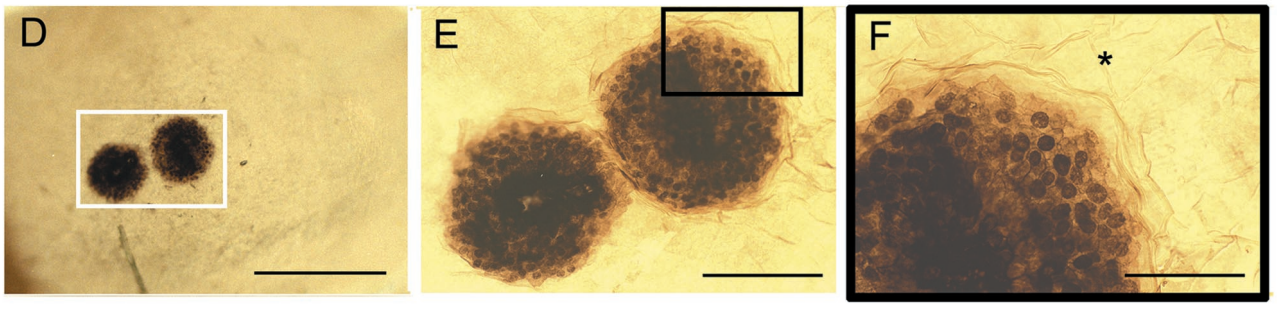

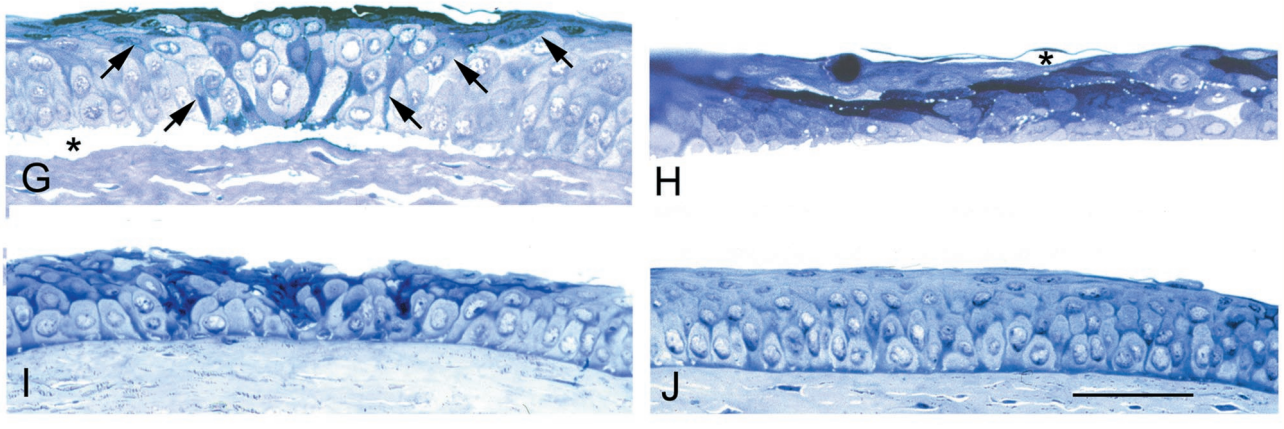

the opposite trigeminal ganglion in that there was no evidence of viral infection. Thus, the small volume of virus that was injected from the micropipette spread to about a 1- to 2-mm radius from the site but spared the majority of cells in the entire trigeminal ganglion.

Satellite cells, which are modified glia-supporting cells characterized by their small nucleus and very close association with neuronal ganglion cell bodies, were also reactive (Fig. 2B). The reactive satellite cells were found both in association with infected neurons and in association with uninfected neurons. Uninfected satellite cells in association with infected neurons were found less frequently. In addition, we found foci of immunostained axons and Schwann cells, defined by their dense nuclear staining and elongate nuclei (Fig. 2B). These areas were infiltrated with few lymphocytes and fewer monocytes.

Control cornea. The structure of normal rodent cornea has been described previously (see reference 3 for a review), and the appearance of areas of non-infected cornea in the current study corresponded to the previous description (Fig. 1, 2J, and 3). The only difference was that there was some surface staining in these otherwise healthy regions of infected cornea (Fig. 3). This was probably the result of HSV products released from areas of infection and cross-linked to the nearby surface during fixation (1).

The majority of the basal cells had a cuboidal shape with relatively lucent cytoplasm and a large oval nucleus (Fig. 3). A minority were more irregularly shaped with a narrower nucleus, and the cytoplasm was more densely populated with a filamentous meshwork (Fig. 3). All of the basal cells contained multiple hemidesmosomes facing the underlying basal lamina (data not shown). Wing cells were easily identified on the basis of their flattened shape, very irregularly shaped nuclei, and ruffled, interdigitating plasma membranes. Adherens junctions were found between basal cells and wing cells, and between squamous cells and wing cells (see Fig. 6B), but not between basal cells. Squamous cells were identified by their thin shape, the darker cytoplasm with more densely packed fibrils in the cytoplasm, and elongate nuclei. Their apical plasma membrane was characteristically ruffled and invaginated into the overlying squamous cells. The most superficial squamous cells were tightly coupled to each other and to the underlying cells.

The axons that innervate the cornea run between the basal cell layer and Bowman's layer, an acellular region of the stromal layer (Fig. 3 and inset) (28). The axons were identified by their more lucent cytoplasm containing large, round mitochondria and by the concentration of small clear vesicles and rare vesicles with dense cores. Additional neuronal profiles were found along the lateral surfaces of basal cells. We did not find any neuronal profiles in contact with squamous cells.

(i) Day 2. HSV was rapidly transported to the peripheral branches of the trigeminal ganglion neurons via anterograde transport to the ipsilateral cornea (Fig. 2C). In one of the five mice infected and euthanized 2 days after inoculation, we found the virus had reached the cornea. We found HSV-immunopositive fibers aligned parallel with the surface of the cornea and running in the superficial quarter of the stromal layer. These fibers were assumed to be trigeminal axons labeled with viral antigen as a result of the trigeminal ganglion inoculation. Basal cells adjacent to the reacted fibers were also lightly stained.

Although we were able to distinguish immunostained trigeminal axons with our light microscopic procedures in which antiserum was applied to permeabilized cells in 10-μm-thick cryosections, we were unsuccessful in identifying patches of infection or incoming axons in whole mounts of corneas prepared for EM. The absence of axons containing HSV antigens may have been due to the penetration problems of the HSV antiserum in whole mounts of cornea or alternatively to the lack of viral antigen expression on the external surface of infected axons.

(ii) Day 3. In animals that were euthanized 3 days after the trigeminal inoculation, we found evidence that the virus had infected a relatively restricted region of the entire corneal surface. Immunopositive cells were not homogeneously distributed across the surface of the cornea but were restricted to patches each about 140 μm in diameter (Fig. 2D and E). Beyond the borders of the patches, adjacent corneal cells were essentially unstained (Fig. 2F). The infected cells formed a circular, raised expansion of the corneal surface. In the center of the patch, each cell's nucleus and cytoplasm were heavily immunostained (Fig. 2E and F). However, at the periphery of the patch, the cytoplasm was only lightly stained, while the nuclei were more darkly stained. The presence of higher concentrations of viral antigens in the nucleus presumably represents the early expression and concentration of immediate-early and early gene products in the nuclear compartment (Fig. 2E and F).

Cross sections through the virus-infected patches showed that a wedge of infected cells had developed in the center (Fig. 2G). The zone of infection extended from the basal membrane up to the corneal surface. Beneath the patch, the adjacent epithelial cells had pulled away from the underlying stroma. In a minority of cases, the entire epithelium in the very center of the patch had pulled away to form an ulcer. The gap between

FIG. 2. (A) Photograph of a longitudinal cryosection through the rostral half of a trigeminal ganglion of a mouse killed 2 days after injection. The section was immunostained with a polyclonal antiserum tagged with horseradish peroxidase. Bar = 150 μm. (B) Photograph of the trigeminal ganglion from the area that contains neurons that innervate the cornea. The plastic-embedded section was immunostained for HSV and counterstained with toluidine blue. Infected cells were stained dark blue (arrow), due to the reactivity of the antibody stain with the toluidine blue stain. Satellite cells (arrowhead) and Schwann cells (chevrons) were also infected. Uninfected neurons were stained light blue (asterisk). Bar = 30 μm. (C) Photomicrograph of a cryosection of the left cornea of a mouse that was euthanized 2 days after inoculation. The patch of infected cornea was seen as brown fibers (arrows) that course along the most superficial portion of the stromal layer (S). A few cells in the epithelial layer (E) were also lightly immunostained. Bar = 15 μm. (D to F) Photographs of an immunostained whole mount of the left cornea from a mouse 3 days after inoculation. The photographs were taken looking down on the surface of the cornea. (D) Two individual patches of infected cells can be seen. Bar = 150 μm. (E) Higher magnification of the region of the cornea indicated by the white box in panel D. In the center of the infection, the nuclei and cytoplasm of infected cells were equally heavily immunoreactive, indicating viral antigens were distributed throughout each cell. Bar = 50 μm. (F) Region of the cornea indicated by the black box in panel E. At the periphery of the patch, the nuclei of infected cells were more darkly immunoreactive than the cytoplasm, indicating that viral antigens were concentrated in the nucleus and had not yet reached significant levels in the cytoplasm. This pattern was indicative of the early stages of infection of cells. Beyond the patch, the corneal cells were not infected (asterisks). Bar = 50 μm. (G to J) Photomicrographs of corneal sections that were immunostained for HSV before fixation and embedding. The sections were counterstained with toluidine blue dye. Bars for G to J = 50 μm. (G to I) Representative sections from serial sections through individual patches of infection. After the each series was examined, the section with the most extensive immunostaining was selected for illustration. (G) Cornea from an animal euthanized 3 days after inoculation. The infected cells formed a wedge from the basal layer to the surface (arrows). The epithelium had separated from the underlying stromal layer at the patch of infection (*) but not beyond those margins. (H) Representative section of cornea from a mouse 4 days after inoculation. The squamous cell layer had blisters (asterisk) as well as clearly necrotic darkly stained cells. The infection had spread widely through the wing and squamous cell layers. (I) Cornea taken 5 days after inoculation. Fewer cells of the basal and wing cell layers were infected, and the squamous cell layer was interrupted and pitted. (J) Section from an uninfected animal. No immunostaining was identified in the cornea.

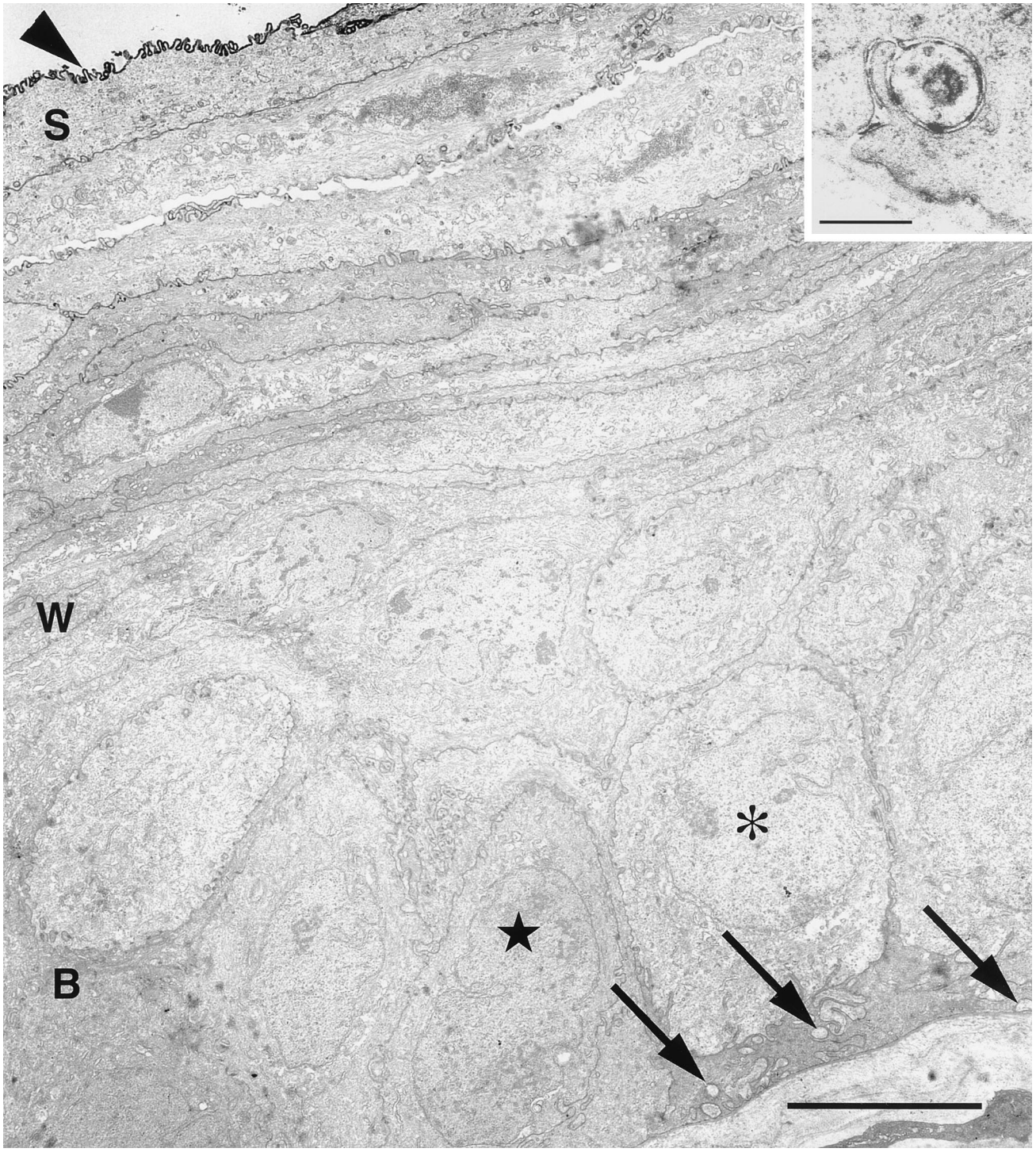

FIG. 3. Electron micrograph of an uninfected region of the corneal epithelium that bordered a patch of infected epithelium from a mouse that was euthanized 5 days after injection of HSV into the trigeminal ganglion. The squamous cell layer (S), wing cell layer (W), and basal cell layer (B) are indicated. At the lower right, the basal cells abut a basal layer. The majority of the basal cells were cuboidal (asterisk); a minority were more irregularly shaped with dense cytoplasm (starred). Embedded in the cytoplasm of the basal cells were clusters of axonal profiles (arrows). The surface of the cornea was coated with HSV antigen, probably as a result of diffusion of viral antigen from a site of infection beyond this field. Bar = 5 μm. (Inset) Higher magnification of axonal profile that invaginated into the base of a basal cell. Bar = 0.2 μm.

the basal layer and stromal layer was limited to the region of the infection and probably resulted from less than normal adhesion between basal cells and stromal cells in this region.

At the EM level, we found that both the large lucent and irregular, denser basal cells were infected with virus and contained both immunoreactive and nonimmunoreactive viral particles (Fig. 4A and B). The dark staining that was characteristic of the borders of the basal cells in the light microscope (Fig.

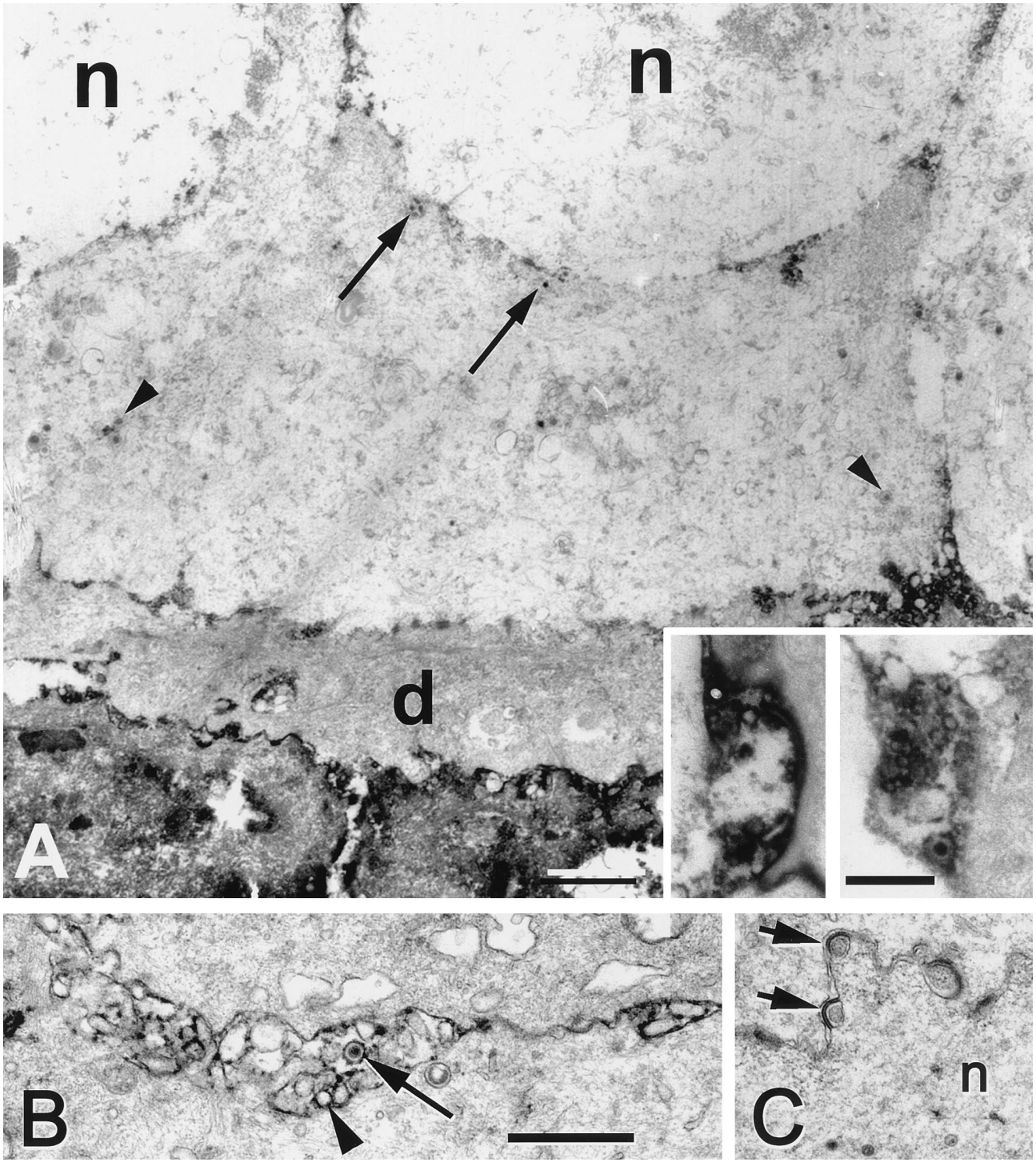

FIG. 4. Electron micrographs showing the basal and wing cells in the cornea 4 days after infection. Bar = 1 μm. (A) Fragment of a darkly stained, degenerating cell is seen in the lower portion, and less densely labeled cells (d) are found immediately above this cell. The more superficial basal cells appeared healthy but contained immature (arrows) and mature (arrowheads) viral particles. (Insets) In the interstices between the basal cells, were seen heavily labeled axons which contained vesicular profiles. The reaction product made differentiation of the inclusions as viral particles or synaptic vesicle difficult, but no structures resembling virions enveloped by a cellular membrane were seen. Inset bar = 0.5 μm. (B) Electron micrograph of portions of two wing cells overlying the basal cells shown in panel A. The cells were lightly immunoreactive, but the cell membranes were more heavily immunolabeled. Incomplete capsids (arrowhead) and a single virion (arrow) were present in the intercellular space. (C) Example of capsids (arrows) exiting the nucleus (n) of a wing cell.

2G) could be seen to be the result of immunoreactive viral antigen that was densely distributed between the cells (Fig. 4A).

We found small unmyelinated axon profiles clustered together in the interstices between the basal cells (Fig. 4A, inset). They generally appeared swollen, and the plasma membrane was often disrupted, as a result of the compromise of ideal fixation for ideal immunogenicity. The nerve fibers were iden-

tified by their small caliber, the presence of multiple vesicles within the profile, and immunoreactivity surrounding vesicles and viral particles. The reaction product largely obscured details of structure within the profiles, which made it difficult to identify definitively single HSV particles (1). In addition to the problem of spread of Ni-DAB reaction product within the axonal compartment, we also were faced with the difficulty of identifying a particle simply on the basis of size. Sensory nerve endings characteristically contain small clear vesicles about 50 to 75 nm in diameter and larger dense core vesicles about 150 nm or more in diameter (10). The immunostained viral particles in axon profiles averaged 91.5 ± 29 nm (n = 22) in diameter (e.g., Fig. 4A, insets).

The overlying wing cells were lightly immunoreactive, with darkly stained material between cells (Fig. 2G). The intercellular space contained immature capsids as well as mature virions (Fig. 4B) that may have been released by cells destroyed by the viral infection. The squamous cells appeared to be the most severely infected cell type.

We identified capsid profiles in the nuclei of infected cells and in some cases found capsid exiting the nuclear envelope (Fig. 4C). The viral capsids in the nucleus was significantly smaller than those found in the cytoplasm of infected corneal cells. Nuclear capsids with DNA and without DNA averaged 99.0 ± 15 nm in diameter (n = 40), whereas those located in the cytoplasm were significantly larger, 138.1 ± 46 nm (n = 11) in diameter. Viral particles that were composed of both an envelope as well as nucleocapsid were frequently enclosed in a cell membrane. These organelles averaged 211.2 ± 18 nm (n = 6) in diameter. There was no preferential release of capsids toward the apical surface. Immature and enveloped virions in cytoplasmic membranes were identified in the cytoplasm of both wing and squamous cells.

(iii) Day 4. In animals that were euthanized 4 days after trigeminal inoculation, the infected patches appeared larger, and the lateral spread of corneal involvement was more extensive. Blistering of the superficial layers of the cornea in the center of an infected patch was more obvious (Fig. 2H), and the entire epithelium was thinner than we had seen in animals that survived 2 or 3 days after infection. By EM, we saw that the basal cell layer was relatively intact, although the cells were obviously infected. Specifically, mature and immature capsids were present in the nucleus of these cells (Fig. 5, upper inset), and enveloped virions were clustered in the extracellular space. In cytoplasmic extensions of basal cells we found clear examples of both individual virions and virions enwrapped in cytoplasmic vesicle membrane (Fig. 5, lower inset). The overlying wing cells contained viral particles in the cytoplasm, and also viral capsids and clumped heterochromatin in the nuclei. There was labeling of the surfaces of wing cells (Fig. 2H). The cytoplasm contained mature and immature virions, and the extracellular space surrounding the squamous cells was also densely immunoreactive. There was no evidence of a polarized delivery of viral product to the apical surface in the cells at this time. The squamous cells located at the center of the patches were also infected, and many nuclei of these cells were densely immunoreactive.

(iv) Day 5. After 5 days, the patches of infection appeared as elongate, finger-like regions, similar to the pattern seen in dendritic epithelial keratitis. The active infection was contained in the squamous and wing cell layers; only these more superficial layers were actively producing virus (Fig. 2I). At the borders of the site of infection, the surfaces of wing cells and some basal cells were HSV positive, which was found to be due to the accumulation of extracellular virus and disposition of viral antigen on the cell surfaces (Fig. 6A). Examination of serial sections through this type of patch revealed no significant ulceration of the cornea. The basal layer remained intact, although an occasional infected basal cell was present.

At the borders of infected patches, it was clear that both HSV-infected squamous and wing cells contributed to the reticulated pattern of staining seen in the whole mounts (Fig. 2I). In these later stages of infection, EM revealed that the plasma membranes of the superficial layer of squamous cells were outlined by a continuous layer of immunostaining, suggesting that viral antigen was more concentrated toward the external surface of the cornea (Fig. 6A). This apical polarization of staining was also seen on the underlying squamous cells as small HSV-positive pits that connected to the apical surface of the cells. No immunopositive pits were identified on the basal surfaces of the cells, nor were any seen on adjacent uninfected squamous cells (Fig. 6B). No evidence of infected basal cells, of infected axonal profiles, or of any extracellular virus was found in the basal layer of the cornea at the borders of the infected patches at 5 days after infection.

Stromal layer. Relatively few keratinocytes were infected with HSV in the stromal layer at any time point (data not shown). The stromal layer was, however, frequently swollen immediately under the infected corneal epithelium. We found no invasion of lymphocytes into the stroma or epithelium by 5 days after infection. Beyond the cornea proper, HSV also infected a few cells in the iris and proximal parts of the ciliary body, but the retina was consistently unstained.

DISCUSSION

In this study, we used a combination of a novel method to deliver virus to the cornea in the whole animal and EM immunocytochemistry to identify the axons and viral particles that are transported and transferred from trigeminal axons to cornea. We report two major findings. First, the initial corneal infection is restricted to basal cells. Despite widespread infection of trigeminal ganglion cells, there is a surprisingly focused spread of HSV preferentially to the basal cell layer of the epithelium. Second, the infection spreads preferentially outward and laterally to the wing and squamous cells and to a lesser extent to the adjacent basal cells.

Neuron to cornea transfer. In previous studies, the delivery of virus from sensory nerve to cornea has been studied after direct infection of the cornea, a necessary feature which unfortunately complicates the analysis of viral spread. Two approaches used direct corneal infection, and they each have resulted in different patterns of epithelial keratitis. Laycock et al. (13) used an approach in which the cornea was primarily infected and then subsequently stimulated with UV-B irradiation to reactivate latent virus in trigeminal neurons and induce transport and recurrent herpetic keratitis. In a related study, Miller et al. (21) compared the patterns of herpetic keratitis that resulted from acute infection of the cornea as a result of scarification and inoculation of virus onto the corneal surface with that resulting from recurrent infection. The major differences were (i) the focal distribution of HSV-1 antigens and (ii) stromal opacification and neovascularization in the recurrent model compared to results in the direct scarification model. By careful consideration of viral load, viral strain and host immunogenetic background, Miller and colleagues were able to eliminate several variables that might contribute to these differences (21). They proposed that two factors might play roles in the evolution of the differences. First, the humoral immunity to HSV in animals undergoing reactivation could act at the level of both the trigeminal ganglia and the cornea and account for the restricted foci of herpetic antigens and destruction in

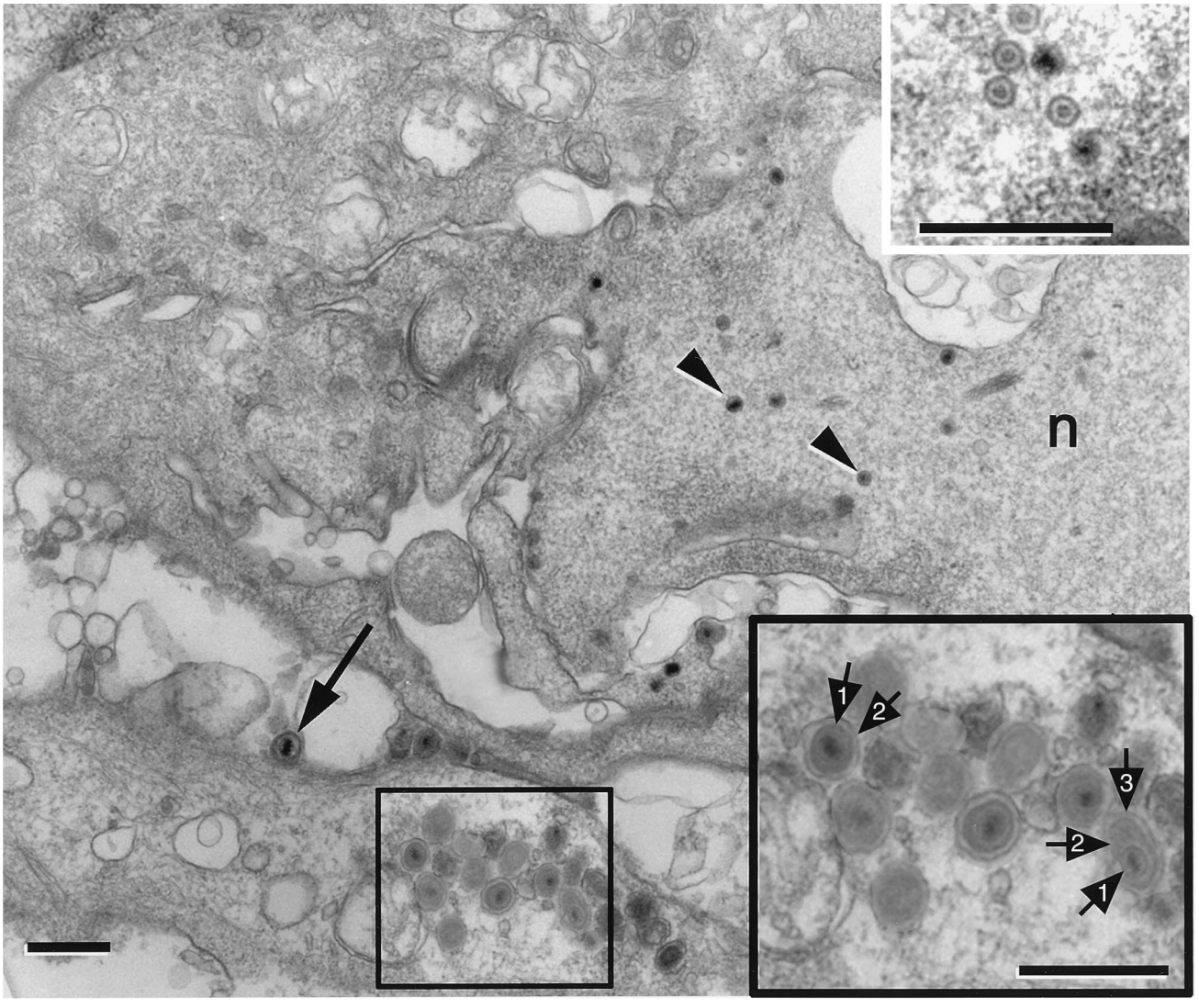

FIG. 5. Electron micrograph of basal cells from an animal that was euthanized 4 days after infection. Mature virions (arrow) were located in the extracellular space. In the lower portion, a cluster of mature virions occupied a process of a basal cell cytoplasm. n, nucleus. Bar = 0.6 μm. (Upper inset) Higher magnification of a cluster of nucleocapsids that were located in the nucleus of the basal cell. Bar = 0.5 μm. (Lower inset) Higher magnification of the boxed area in Fig. 5. These mature virions were comprised of a capsid (1) and a distinct envelope (2). One of the virions was enclosed in a cellular membrane (3). Bar = 0.75 μm.

the recurrent model. Second, the potentially limited number of latently infected neurons that could be reactivated could also limit the size and/or number of foci.

Our results suggest that at least for the first 5 days after reactivation of virus in the recurrent infection, the focal delivery of virus to topographically limited regions of the cornea from individual infected trigeminal ganglion neurons may account entirely for these major differences. As a result of directly infecting trigeminal ganglion neurons, we found a focal distribution of HSV antigens. Since the trigeminal axons are the only possible source of virus in our study, the subbasal nerve plexus must generate the infection. This finding supports previous studies that suggested this as the source of the distribution of epithelial lesions in human patients (16, 26).

In an earlier study, we used EM immunocytochemical procedures to define the intracellular compartments occupied by HSV in infected trigeminal ganglion cell bodies (10). In these neuron cell bodies, the HSV-immunoreactive organelles were composed of three concentric layers, including capsid, envelope, and cellular membrane. In the present study, we found that the immunostained viral particles in the axons innervating the corneal epithelium were significantly smaller, about 100 nm in diameter. They were also significantly smaller than either mature virions seen in the extracellular space or in corneal epithelial cells in this study. Although our results are only preliminary due to the difficulties in identifying membrane limits in immunostained tissue and the small numbers of observations, our results support the model of anterograde transport of HSV developed by Penfold et al. (23).

Spread within the cornea. The mechanism of expansion and elaboration of the lesions within the cornea remains to be defined precisely. However, it is clear that cells of all three layers of the epithelium became infected at the early stages and may or may not be sloughed off to form an ulcer. Whether this ulceration results from the separation of epithelium from stroma at the early stages, from the distortion of the normal innervation pattern and potential destruction of sensory nerve

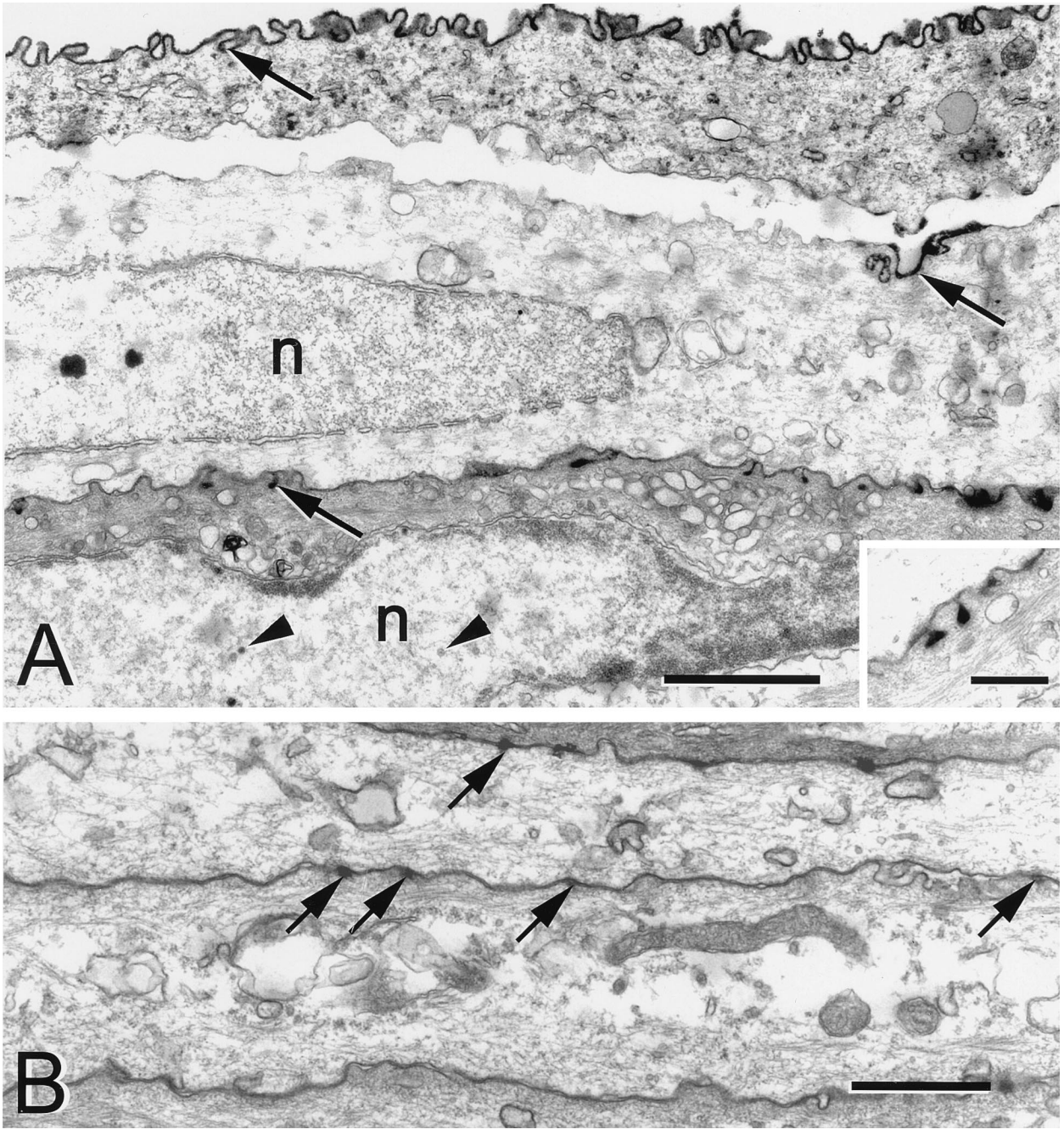

FIG. 6. Electron micrographs of squamous cells from a mouse 5 days after HSV injection into the ipsilateral trigeminal ganglion. (A) The apical plasma membranes of the squamous cells were coated with viral antigen (arrows). The basal surfaces were relatively free of viral antigen. Capsids (arrowheads) were found in the nucleus (n). Bar = 1.0 μm. (Inset) Higher magnification of the HSV positive pits present on the apical surface of a squamous cell. Bar = 0.25 μm. (B) Photomicrograph of the squamous cells from an uninfected region of the same cornea. There was no immunostaining in the cells. Only an occasional membrane invagination was seen along the outer surface of the cell. Arrows indicate adherens junctions. Bar = 1.0 μm.

endings as a result of viral release, or some other combination of factors is unknown.

By 5 days after infection, we found evidence of the rapid repopulation of the epithelium with basal cells that were free of capsids or mature virions. Intact axons were also found adjacent to basal cells. This apparent rapid remodeling and reinnervation of the basal cells by sensory axons resembled the plasticity of sensory nerve endings described by Harris and Purves in their model of living mouse cornea (4).

The lateral spread of virus in the wing and squamous cell layers is due to a combination of factors including the geometry of broader cell shapes and the polarized transfer of virus from the apical surface of one cell to the basal surface of the overlying cell. Additional evidence that neuronal innervation is not required for the lateral spread of infection in the corneal epithelium comes from recent in vitro studies (7, 27). Corneal epithelial cells with no neuronal contribution can be induced to differentiate into a complex, multilayered epithelium by grow-

ing the cells in organotypic raft cultures. When these cells are infected with HSV, the virus spreads laterally in the epithelial layer, similar to that seen in our animal model.

Our unexpected finding in vivo of a polarized delivery of viral antigen between corneal epithelial cells first seen 5 days after viral inoculation of the trigeminal ganglion extends previous work done in vitro (5) in which newly synthesized HSV was targeted to the apical surface of MDCK cells. To our knowledge, ours is the first in vivo description of a polarized expression of HSV in nonneuronal cells. The identities of the viral antigens that contribute to corneal plasma membrane labeling remain to be determined. This preferential delivery of new virus and viral proteins to the apical surface of the cornea may also serve to facilitate the rapid release of new virus into the tear film, as well as protect virions and virally infected cells from complement-mediated neutralization. If so, it is a relatively late mechanism, since we did not find equivalent immunoreactive pits at 2, 3, or 4 days after infection. It may also serve to reduce the concentration of virus that accumulates at the base of the epithelium adjacent to Bowman's membrane. This layer contains a high concentration of complex sugars that would bind excess virus and impede its egress from the epithelium.

Animal model. In our study, there was a rather limited zone of cornea that became infected, despite the fact that at least one-fifth of the trigeminal ganglion ultimately became infected with virus over the course of the 5-day postinfection period. The limited corneal involvement that results in the recurrent infection model of Laycock et al. probably rests, in part, on the limited number of ganglion cells that become latently infected and subsequently reactivate with any one stimulus (13; see also reference 24). Only 60 to 80% of the animals infected in Laycock's model demonstrate viral reactivation, and for each animal there is no information about the number of ganglion cells that this represents. The direct injection results in a large number of infected ganglion cells. Another factor in the recurrent model is that the delivery of virus by direct corneal inoculation and retrograde transport involves several possible sources of reactivated virus in other ganglia, e.g., sympathetic and parasympathetic ganglion cells. From the results of the present study, we conclude that autonomic involvement is apparently not essential for the development of a focally restricted herpetic infection of the cornea, since only sensory neuron cells were directly infected.

There were obviously significant differences in the route of delivery of virus in our model and that of previous animal models. The difference was most clearly illustrated in the appearance of unimmunostained ganglion cell bodies that were frequently found surrounded by immunostained satellite cells in the trigeminal ganglion. This is in contrast to the pattern of HSV-infected neurons in the trigeminal ganglion that was observed in our earlier study of primary scarification and corneal inoculation with HSV-1 (11). In this earlier study, we found a more consistent pairing of infected satellite cells with neighboring infected ganglion cells. Direct inoculation of virus into the trigeminal ganglion spreads in the extracellular space of the ganglion, where it is directly available to Schwann cells and satellite cells, but only indirectly through transfer via the satellite cells to the trigeminal neuron cell bodies. By contrast, virus delivered to nerve terminals in the cornea is transported to the neuron cells bodies and only secondarily is available to satellite and Schwann cells.

We cannot distinguish the mode of viral maturation in corneal cells. In those cells we found a variety of viral morphologies in the cytoplasm, ranging from nucleocapsids with no envelope to fully enveloped virus in a host cell membrane compartment (Fig. 5, inset). One possible argument would be that transport of virus from nucleus to cell surface of a corneal cells does not require the specialized transport features characteristic of axonal delivery (23).

In sum, we have developed a novel animal model to study the mechanisms of delivery of HSV-1 in viral infections of the cornea. The strengths of the model are the greater control over the amount of virus delivered, the time course of infection, and elimination of confounding factors such as the potential contribution of virus from latently infected cornea or conjunctival sources. The major limitation of the model is the requirement of stereotaxic equipment for the surgical approach to directly deliver HSV to the trigeminal ganglion. Our goal was to investigate how HSV synthesized in trigeminal ganglion neurons would be delivered to axon endings in the cornea and spread to the epithelial cells. We have not attempted to mimic directly the delivery of HSV from infected and reactivated neurons. Although virus released to the extracellular space from reactivated neurons might arrive at other ganglion cells in a similar fashion, it would be difficult, if not impossible, to know the precise concentration of virus that is released from latently infected cells. Further development of the model should include priming of the host immune system with HSV antigens, in order to determine more accurately the role of this system in stromal and epithelial opacification. Last, using this model, the contribution of different viral gene products to viral release by neurons as well the transfer of virus from cell to cell in the corneal epithelium can now be addressed.

ACKNOWLEDGMENTS

This work was supported by PHS grants EY-08773 and P30 EY02162 (J.H.L.) and NS 23347 and NS 21445 (P.T.O.), by funds from That Man May See, Inc. and Fight for Sight, and by a REAC grant from UCSF.

We acknowledge Nerissa Mendoza and Kate Wall for excellent technical assistance and Walter Denn and Erin Browne for graphics assistance. We are also grateful to T. Mauro, K. Topp, T. P. Margolis, and L. Müller for valuable discussions.

REFERENCES

1. **Courtoy, P. J., D. H. Picton, and M. G. Farquhar.** 1983. Resolution and limitations of the immunoperoxidase procedure in the localization of extracellular antigens. J. Histochem. Cytochem. **31:**945–951.
2. **Crouse, C. A., S. C. Pflugfelder, I. Pereira, T. Cleary, S. Rabinowitz, and S. S. Atherton.** 1990. Detection of herpesviral genomes in normal and diseased corneal epithelium. Curr. Eye Res. **9:**569–581.
3. **Gipson, I. K., and S. P. Sugrue.** 1994. Cell biology of the corneal epithelium, p. 1–13. *In* D. M. Albert and F. A. Jakobiec (ed.), Principles and practice of ophthalmology. Lippincott, Philadelphia, Pa.
4. **Harris, L., and D. Purves.** 1989. Rapid remodeling of sensory endings in the corneas of living mice. J. Neurosci. **9:**2210–2214.
5. **Hayashi, K.** 1995. Role of tight junctions of polarized epithelial MDCK cells in the replication of herpes simplex virus type 1. J. Med. Virol. **47:**323–329.
6. **Holland, D. J., M. Miranda-Saksena, R. A. Boadle, P. Armati, and A. L. Cunningham.** 1999. Anterograde transport of herpes simplex virus proteins in axons of peripheral human fetal neurons: an immunoelectron microscopy study. J. Virol. **73:**8503–8511.
7. **Hukkanen, V., H. Mikola, M. Nykänen, and S. Syrjänen.** 1999. Herpes simplex virus type 1 infection has two separate modes of spread in three-dimensional keratinocyte culture. J. Gen. Virol. **80:**2149–2155.
8. **Kaufman, H. E.** 1978. Herpetic keratitis. Investig. Ophthalmol. Vis. Sci. **117:**941–957.
9. **LaVail, J. H., S. Rapisardi, and I. K. Sugino.** 1980. Evidence against the smooth endoplasmic reticulum as a continuous channel for the retrograde axonal transport of horseradish peroxidase. Brain Res. **191:**3–20.
10. **LaVail, J. H., L. B. Meade and C. R. Dawson.** 1991. Ultrastructural immunocytochemical localization of herpes simplex virus (type 1) in trigeminal ganglion neurons. Curr. Eye Res. **10**(Suppl.)**:**23–29.
11. **LaVail, J. H., K. S. Topp, J. A. Garner, and P. A. Giblin.** 1997. Factors that contribute to the efficiency of transneuronal spread of herpes simplex virus. J. Neurosci. Res. **49:**485–496.
12. **LaVail, J. H., J. Zhan, and T. P. Margolis.** 1990. HSV (type 1) infection of the trigeminal complex. Brain Res. **514:**181–188.

13. **Laycock, K. A., S. F. Lee, R. H. Brady, and J. S. Pepose.** 1991. Characterization of a murine model of recurrent herpes simplex viral keratitis induced by ultraviolet B radiation. Investig. Ophthalmol. Vis. Sci. **32:**2741–2746.
14. **Liesegang, T. J.** 1989. Epidemiology of ocular herpes simplex. Incidence in Rochester, MN, 1950–1982. Arch. Ophthalmol. **107:**1155–1159.
15. **Llewellyn-Smith, I. J., P. Pilowsky, and J. B. Minson.** 1993. The tungstate-stabilized tetramethylbenzidine reaction for light and electron microscopic immunocytochemistry and for revealing biocytin-filled neurons. J. Neurosci. Methods **46:**27–40.
16. **Lohmann, A. M., L. J. Müller, E. Pels, P. G. H. Mulder, and L. Remeijer.** 1999. Corneal epithelial nerves are the anatomic basis for the dendritic figure caused by herpes simplex virus. Investig. Ophthalmol. Vis. Sci. **40:**S549.
17. **Lumb, W. V.** 1963. Small animal anesthesia. Lea and Febiger, Philadelphia, Pa.
18. **Lycke, E., K. Kristensson, B. Svennerholm, A. Vahlne, and R. Ziegler.** 1984. Uptake and transport of herpes simplex virus in neurites of rat dorsal root ganglia cells in culture. J. Gen. Virol. **65:**55–64.
19. **Margolis, T. P., B. Togni, J. H. LaVail, and C. Dawson.** 1987. Identifying HSV infected neurons after ocular inoculation. Curr. Eye Res. **6:**119–126.
20. **McLean, I., and P. Nakane.** 1974. Periodate-lysine paraformaldehyde fixative. A new fixative for immunoelectron microscopy. J. Histochem. Cytochem. **22:**1077–1083.
21. **Miller, J. K., K. A. Laycock, J. A. Umphress, K. K. Hook, P. M. Stuart, and J. S. Pepose.** 1996. A comparison of recurrent versus primary HSK in inbred mice. Cornea **15:**497–504.
22. **Pavan-Langston, D.** 1994. Viral disease of the cornea and external eye, p. 117–147. *In* D. M. Albert and F. A. Jakobic (ed.), Principles and practice of ophthalmology. Lippincott, Philadelphia, Pa.
23. **Penfold, M. E. T., P. Armati, and A. L. Cunningham.** 1994. Axonal transport of herpes simplex virions to epidermal cells: evidence for a specialized mode of virus transport and assembly. Proc. Natl. Acad. Sci. USA **91:**6529–6533.
24. **Sawtell, N. M.** 1997. Comprehensive quantification of herpes simplex virus latency at the single-cell level. J. Virol. **71:**5423–5431.
25. **Stanberry, L. R.** 1992. Pathogenesis of herpes simplex virus infection and animal models for its study. Curr. Top. Microbiol. Immunol. **179:**15–28.
26. **Tabery, H. M.** 1998. Early epithelial changes in recurrent herpes simplex virus keratitis. Acta Ophthalmol. Scand. **76:**349–352.
27. **Visalli, R. J., R. J. Courtney, and C. Meyers.** 1997. Infection and replication of herpes simplex virus type 1 in an organotypic epithelial culture system. Virology **230:**236–243.
28. **Whitear, M.** 1960. An electron microscope study of the cornea in mice, with special reference to the innervation. J. Anat. **94:**387–409.
29. **Whitley, R. J.** 1996. Herpes simplex virus, p. 2297–2342. *In* B. N. Fields (ed.), Fields virology. Raven Press, New York, N.Y.
30. **Whitley, R. J., D. W. Kimberlin, and B. Roizman.** 1998. Herpes simplex viruses. Clin. Infect. Dis. **26:**541–553.